Geofísica Internacional (1992), Vol. 31, Num 4, pp. 341-358

Reconnaissance electrical resistivity and self-potential studies of the Atotonilco-Jonacatepec region, Morelos State, Mexico

J. Urrutia-Fucugauchi*

Laboratorio de Paleomagnetismo y Geofísica Nuclear, Instituto de Geofísica, U.N.A.M., México.

**Collaboration of Electrical Prospecting Group: Martin Bremer, Octavio Orozco, Carlos Flores, Enrique Lima and Students of the Course of Electrical Prospecting, Geophysical Engineering, Faculty of Engineering, UNAM, Mexico.*

Received: 19 June, 1991; accepted: 19 November, 1991.

RESUMEN

Se presentan resultados preliminares de un estudio geofísico en la región de Atotonilco-Jonacatepec, Estado de Morelos. Los resultados de sondeos eléctricos verticales con la configuración electródica de Schlumberger y de potencial natural (SP) permiten delinear la estructura subsuperficial de las unidades volcanoclásticas y lahares y los cuerpos intrusivos. La zona presenta un interés desde varios aspectos tales como geohidrología, geotermia y geología estructural. Se analizan datos para 51 sondeos de 300 m a 400 m de AB, 6 sondeos de 600 m de AB y 10 sondeos de 1000 m de AB, distribuídos en tres perfiles que cruzan la región. La mayor parte de los sondeos se han interpretado con modelos simples de 3 y 4 capas horizontales y sólo la mitad de los sondeos más largos requieren de modelos con un mayor número de capas. Las profundidades máximas modeladas están en el rango de unos 150 a 250 m. Las resistividades aparentes de las unidades volcanoclásticas varían entre los perfiles y algunas capas delgadas aparentemente no se han identificado en todos ellos. Las capas más profundas 4 y 5 corresponden a las unidades carbonatadas Cretácicas. Las capas intermedias 2 y 3 corresponden a los depósitos de lahar y a las volcanoclásticas de las formaciones Tlayecac y Cayuca. Las capas superficiales son material pobremente consolidado con grados variables de saturación de agua y caracterizado por un rango amplio de resistividades aparentes. La continuación en el subsuelo de los cuerpos intrusivos de Jantetelco parece ser más profunda de 150 m. Las anomalías de potencial natural son negativas y parecen formar parte de anomalías dipolares de mayor amplitud. Estas anomalías podrían estar asociadas a movimientos regionales ascendentes de fluidos y anomalías térmicas cerca y en los cuerpos intrusivos. La fuente de calor para los manantiales calientes en la región no ha sido documentada. Esta puede estar relacionada a los intrusivos y contribuir a la generación de las anomalías dipolares de potencial natural. Estudios limitados se realizaron también sobre una pequeña caverna en calizas cerca de Cocoyoc y en la zona de falla regional del Cañón de Lobos. La cueva está caracterizada por altas resistividades aparentes, que delinean la proyección en superficie de la cueva. Partes más profundas que 4 a 5 m no pudieron ser detectadas. Los sondeos sobre la zona de fallamiento están caracterizados por bajas resistividades aparentes y curvas Schlumberger casi planas.

PALABRAS CLAVE: Sondeos de resistividad, potencial natural, Estado de Morelos, energía geotérmica, México.

ABSTRACT

Preliminary results of a geophysical study of the Atotonilco-Jonacatepec area (Morelos State) using DC-resistivity and self-potential (SP) soundings, are used to outline the shallow underground structure of the volcanoclastic and lahar units and the intrusive bodies. Fifty-one 300 to 440 m-AB, six 600 m-AB and ten 1000 m-AB vertical soundings with the Schlumberger configuration were completed along three profiles. Most of the soundings could be interpreted by 3 to 4 layer models, but half of the 1000 m-AB soundings suggest more complex (multi-layered) structures. Maximum depths are of 150 to 250 meters. Deeper layers 4 and 5 may correspond to limestone; layers 2 and 3 may correspond to lahar deposits and sediments of the Tlayecac and Cayuca formations; and the surficial layer corresponds to unconsolidated material. The subsurface continuation of the Jantetelco granodiorites seems to be deeper than 150 meters. The SP anomalies are negative and appear to form part of larger dipolar anomalies. They may result from upwelling where regional southward flow approaches the intrusive bodies. Limited studies conducted over a limestone cave near Cocoyoc feature high apparent resistivities, which outline the surface projection of the cave entrance; parts of the cave deeper than 3-4 m proved difficult to detect. Soundings in a fault zone near Cañón de Lobos above volcanoclastic and alluvial sediments feature very low resistivities and almost flat Schlumberger apparent resistivity curves.

KEY WORDS: Resistivity soundings, self-potential, Morelos State, geothermal energy, Mexico.

INTRODUCTION

During the last few years considerable attention has been given to the exploration of potential sources of geothermal energy as a viable alternative to the use of hydrocarbons and radioactive materials. In Mexico, studies have been focussed on mainly two areas, both linked to plate tectonic boundaries. One area belongs to the San Andreas transform fault system and the spreading centres within the Gulf of California while the other is sited in the Mexican volcanic belt (Figure 1).The first economic geothermal plant of Mexico in operation is in Baja California near the border with the United States (Cerro Prieto, 700 MW). Priority now goes to the second area because of its apparent greater potential and also because of the higher energy demand in and around Mexico City.

Mexico City is located within the volcanic belt; part of the city is built on lava flows. In fact the entire metropolitan area lies in a basin formed by volcanic structures, which

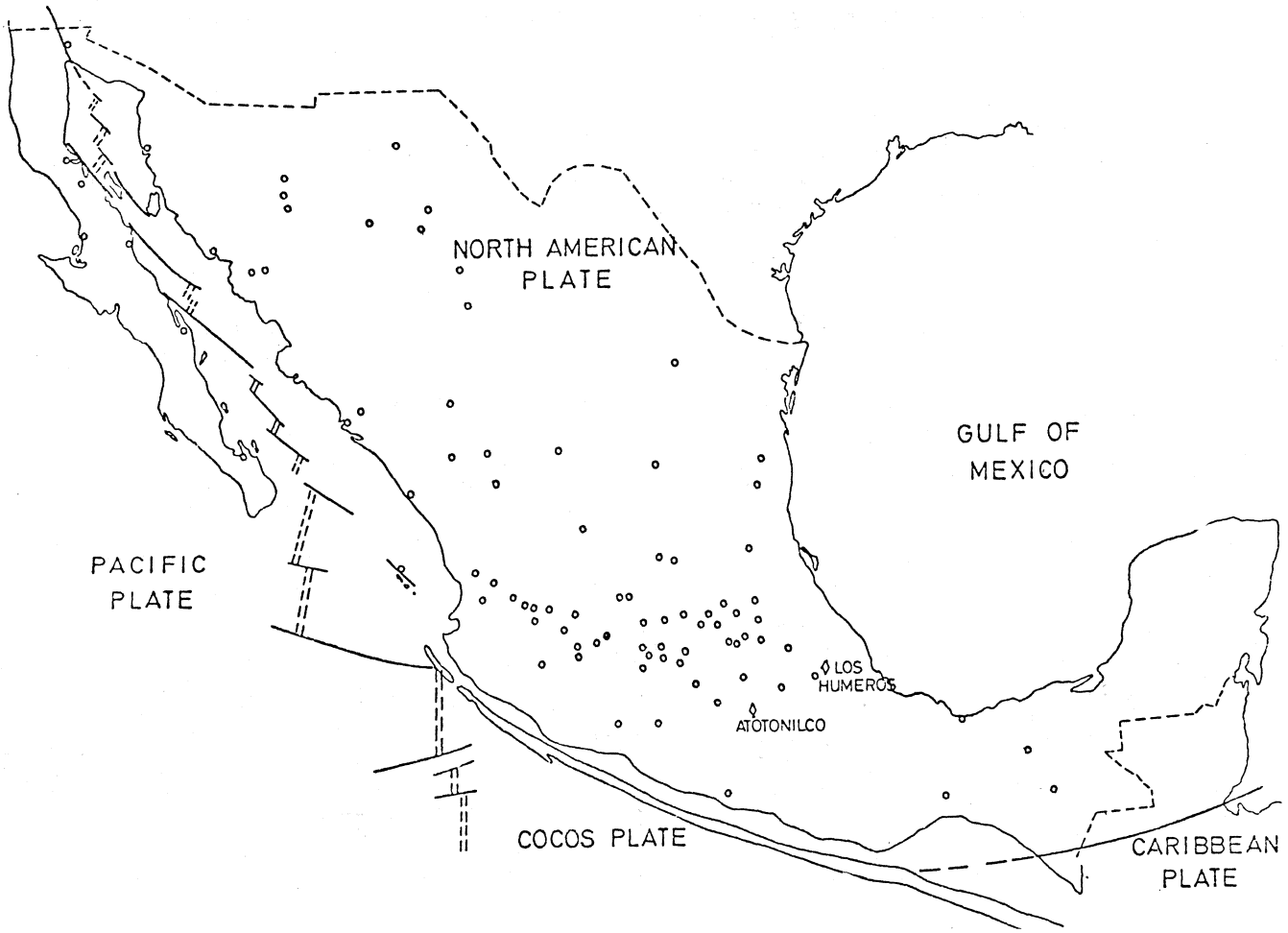

Fig. 1. Location of geothermal manifestations (open circles). The study area is marked by an open rhomb (Atotonilco). Note the concentration of manifestations in the central part, oriented roughly east-west, which corresponds to the province of the Trans-Mexican Volcanic Belt.

include Popocatépetl and Iztaccihuátl, both well above 5000 m altitude. To the south of the volcanoes, at the southern edge of the Mexican Volcanic belt, lies an area of hot-water springs (Figure 1). The present study is concerned with a sector of this zone, to the south of Cuautla and around Jonacatepec and Atotonilco (Figure 2).

The area of Atotonilco-Jonacatepec (Figure 2) was selected for a geoelectric study because of (a) geothermal activity and the need for evaluating its geothermal potential, (b) the need for understanding the geohydrology of the area, and (c) an interest in its shallow surface structure (i.e. configuration of the intrusive bodies). Apart from several deep gullies and the intrusive highs the region is almost flat. It is ideally suited for geoelectric studies. The area to the west contains a variety of karstic structures and some major regional faults, which are also accessible to geoelectrical methods. We describe the results of a combined (SP) self-potential and direct current (DC-) resistivity survey over the area, and we discuss the results of a paleomagnetic and rock-magnetic study previously carried out in the Jantetelco Granodiorites and the Tepexco Volcanic Group (Urrutia-Fucugauchi, 1981).

Rock units in the area are mostly Cretaceous limestones (Figure 2b). The Cretaceous is folded and the regional major faults may be seen mainly to the west. Surveys of a limestone cave near Cocoyoc and across a fault zone in Cañón de Lobos are also described. This was included in order to calibrate the DC resistivity response of the structures and their possible relationship or implications for the main study area. The results show some interesting aspects on detection capability of the Schlumberger dipolar configuration for shallow cavities, and the apparent no-contrast flat resistivity curves over a lateral fault zone.

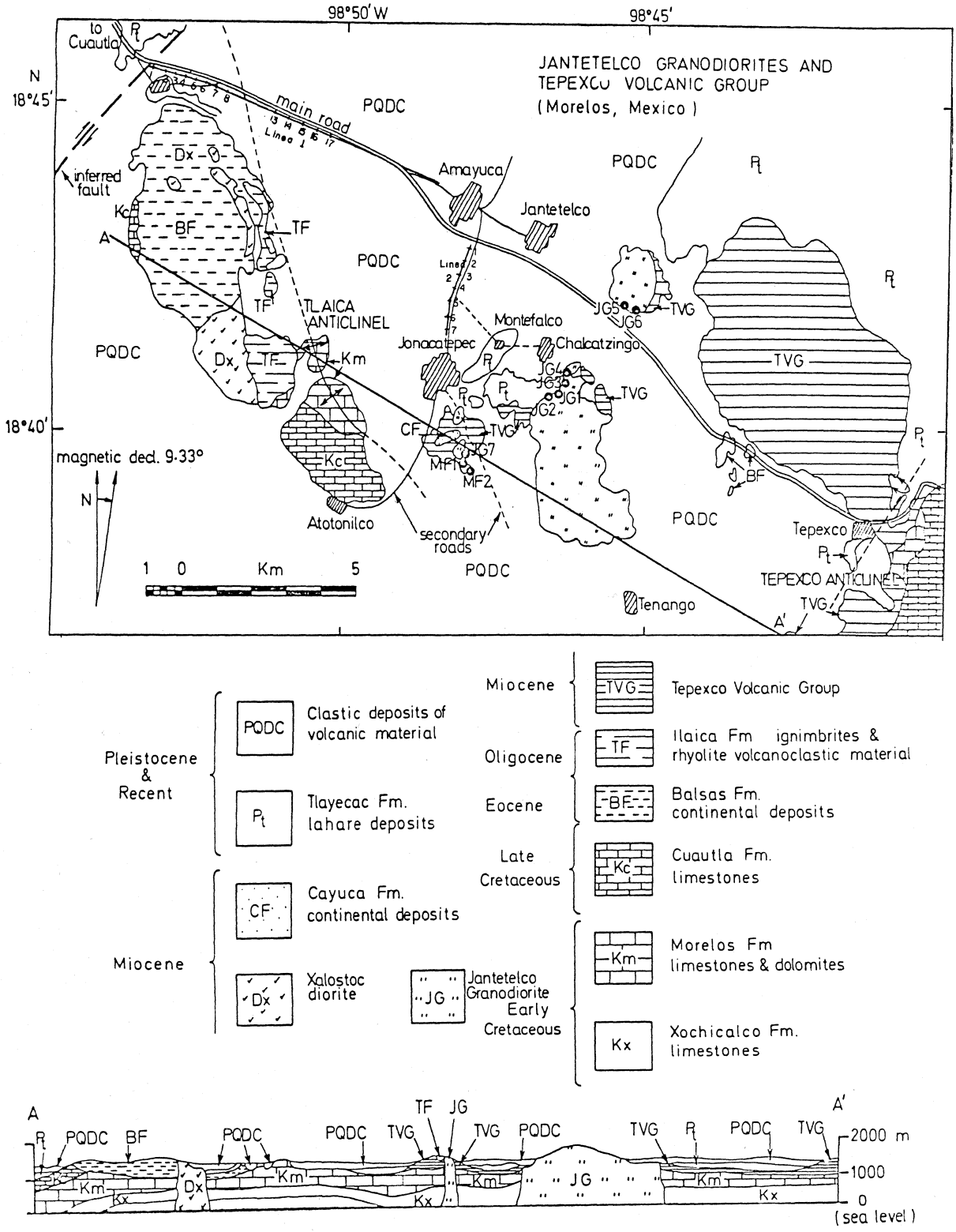

Fig. 2. a) Simplified geologic map of the study area in the State of Morelos (after Fries, 1965). Location of self-potential and resistivity profiles is indicated by the continuous lines (Lines I, II and III). Line I has been subdivided into two segments at approximately the intersection of the Tlaica anticlinel. Stratigraphic column and symbol explanation is in (b).Also shown is a interpreted geological cross-section (labelled A-A') by Fries (1965). The closed dots with identifications JG1 to JG6 and MF1 and MF2 correspond to the paleomagnetic sampling sites.

GEOLOGIC SETTING

The region is situated between 18° 36'N and 18° 45'N and 98° 44'W and 98° 50'W (Figure 2a.). The Panamerican Highway and several secondary roads provide easy access to the villages of Jonacatepec, Amayuca and Atotonilco. Topographic highs correspond to the intrusive bodies of the Jantetelco granodiorites (oriented NNE) and to the composite range of the Xalostoc diorites (oriented NNW). Elsewhere the terrain is relatively flat, with a regional tilt to the south which controls the hydrological conditions in the region. The Popocatépetl-Iztaccihuátl volcanic complex rises to the north.

The oldest outcrops in the area belong to the Morelos Formation, of Albian-Cenomanian age. This is followed by the Cuautla Formation of Turonian age, resting on top of the Xochicalco Cretaceous limestone (not exposed in the area), of Neocomian-Aptian age (Figure 2b). The Mexcala Formation is covered by the Balsas Formation which includes continental clastic, volcanic and lacustrine sediments. Its age may range from the Late Eocene to the early Late Oligocene, De Cserna (1965). The Balsas Formation overlies unconformably the Mexcala Formation: it is interpreted as a continental molasse deposit (de Cserna, 1965). In turn it is conformably overlain by rhyolites and latites of the Tlaica Formation. To the west, the igneous rocks are assigned to the Tilzapotla Formation which has been dated by the Pb -x method at 26 Ma (Jaffe *et al.*, 1959) and by K/Ar on whole rock at 49 ± 3 Ma (Linares and Urrutia-Fucugauchi, 1981). The age of the Tlaica-Tilzapotla Formation is believed to be Eocene-Early Oligocene (see also comments in Urrutia-Fucugauchi, 1983). This formation is covered by lava flows and volcanoclastic deposits of the Miocene Tepexco Volcanic Group. Chemical analyses indicate rhyodacites, dacites and andesites for some units. The next unit, of probable Late Miocene age, is the Cayuca Formation formed by lake deposits. It is of limited extent. In some areas, these lavas and sediments are pierced by intrusive bodies which belong to the Miocene, since they are covered by Pliocene units (Fries, 1965). The intrusives may however be younger, as indicated by unpublished radiometric dates (R. Armstrong, University of British Columbia, pers. communication, 1982). More detailed dating of the igneous activity is considered necessary in order to evaluate the geothermal potential of the region.

The intrusive bodies are assigned to two groups, the Tlaica or Xalostoc Diorites and the Chalcatzingo or Jantetelco Granodiorites (Figure 2b). The Jonacatepec Granodiorites consist of four bodies piercing the Tepexco Volcanic Group (Figure 2). Next comes the volcanic complex of the Popocatépetl volcano and the Tlayecac Formation. The latter is formed by lahar deposits which are interbedded with the Popocatépetl lava flows near the flanks of the volcano. Finally, most of the surface is covered by continental clastic deposits formed mainly by volcanic material and alluvium (Figure 2a,b).

The region is part of the Balsas-Mexcala Basin. Drainage is to the south, by the Las Palmas river and partly by the Tepaltzingo river which flows into the Balsas-Mexcala system. To the west of the area, drainage is by the Amacuzac, Chinameca and Yautepec rivers. There are many all-year streams, springs and some lakes. The karstic topography includes several caves, underground currents, 'dolinas' and 'polyes'. The Tequesquitengo lake southwest of Cuautla is in one of the larger 'polyes'. In general, the area is in an advanced geomorphologic maturity stage, with wide alluvial plains and a well developed drainage system (Fries, 1965).

Annual precipitation exceeds 750 mm and the average monthly mean temperature is above 18°C. Winters are dry and rain is common the rest of the year. To the north of the area there is a region of low rainfall to the south of the Popocatépetl volcano. Rainfall in Cuautla just west of the area, is about 640 mm per year. Water supply is a problem.

GEOPHYSICAL DATA

The major hot-water springs are in the Atotonilco, Tepexco and Tenango villages and near the eastern and western flanks of the larger body of Jantetelco Granodiorites (Figure 2a). A major difficulty in interpreting the area is that the underground structure is poorly documented. Thus the four bodies of the Jantetalco Granodiorites may represent the outcrops of a single deep intrusive which might also constitute the high-temperature source of the geothermal activity. The magmatic activity, age and thermal (and cooling) conditions of the heat source are all unknown.

SELF-POTENTIAL AND DIRECT-CURRENT RESISTIVITY SURVEYS

Surveys of geothermal areas by self-potential and direct-current (DC) resistivity methods are extensive and worldwide (e.g. Zohdy, *et al.*, 1973; Anderson and Johnson, 1976; Stanley *et al.*,1976; Tripp *et al.*, 1978; Corwin and Hoover, 1979; Orellana, 1982). These methods can provide useful data on the underground structure and on hydrologic conditions and the geothermal activity. The area around Jonacatepec village (Figure 2) is well suited to these methods because (1) the topography is relatively smooth, (2) there are surface geothermal manifestations, (3) the access is easy, and (4) the underground structure appears to be relatively simple. Thus it was hoped that problems often encountered in electrical surveys (Kunetz, 1966; Keller and Frischknecht, 1966; Orellana, 1982) would be minor.

Self-potential results

Self-potential measurements were carried out with a high-impedance multi-voltmeter (Scintrex International Limited) and an electrode spacing of 200-300 m. The profiles are shown in Figure 2a. (L-I, L-II and L-III). Because of the large area of the survey the potential gradients were

measured along profiles which were later added on and referred to selected base stations. Polarization and drift were not monitored during the work, and no corrections were applied for these effects. However, the relative position of the electrodes was reversed for alternate readings in order to compensate for electrode potential imbalance, and some care was taken to ensure small electrode contact resistance and small potential difference due to the electrode-connections-wire system.

Perhaps a more important source of disturbance is the occurrence of stray currents due to power lines, rusting pipelines and other iron sources. Such SP effects can range from irregular spikes to sinusoidal or square waves of high amplitude (Corwin and Hoover, 1979). For instance, the water supply to the villages runs close to the profiles studied. In the case of Jonacatepec, rather strong noises were a matter of concern for the residents due to problems with the old pipeline water-supply system.

The self-potential data are summarized in Figure 3. The most outstanding results are the pronounced negative anomalies, which seem to belong to larger dipolar anomalies. Line I (Figure 3a) shows two negative anomalies of about 40 mV; the larger one approaches -57 mV and shows a net potential difference of over 67 mV across a distance of about 4 km. Negative anomalies were found in other areas associated with the Tlaica anticlinal: they may reflect a near-surface water table. They are possibly associated with high temperature and flow of subsurface fluids. The gradient shows two negative anomalies which correlate with the minimum values of the self-potential data (Figure 3a), plus some positive anomalies. The latter may be due to water table variations, or to local changes in water circulation and temperature patterns. Some possible mechanisms of self-potential anomalies generated by geothermal activity have been reviewed by Corwin and Hoover (1979). They propose two main mechanisms, namely thermoelectric coupling due to a thermal gradient across a rock unit, and electrokinetic coupling (or streaming potential) due to fluid flow through porous media. In our study it is difficult to identify a mechanism for the generation of the SP anomalies; both mechanisms may be acting, i.e. a thermal anomaly and fluid flow in the sedimentary units and a thermal gradient across the intrusive bodies.

The results from profiles L-II (Figure 3b) and L-III (Figure 3c) also show pronounced dipolar anomalies. The net differences for L-II is over 60 mV across a distance of about 1.5 km and for L-III more than 40 mV across a distance of about 1 km. The similarity of the anomalies suggests that a common source may be responsible. It may be inferred that the source is deeper for profile L-I than for profiles L-II and L-III.Conversely, the amplitudes suggest that the mechanism responsible for anomalies may be acting more strongly beneath profiles L-I and L-II than beneath profile L-III. These results appear to correlate with the location of the granodiorite bodies (which are nearer profiles L-II and L-III); however, profile L-III located between the two major intrusive bodies (Figure 2) shows the smaller self-potential and gradient anomalies.

Direct-current resistivity soundings

Direct-current (DC) resistivity soundings were carried out using a Scintrex RSP-6 resistivity meter. The Schlumberger electrode configuration was used for its advantages in terms of resolution along traverse lines (Kunetz, 1966; Orellana, 1982). A total of fifty-one 300 to 440 m-AB, six 600 m-AB and ten 1000 m-AB deep soundings were completed along three traverses. The electrode configuration of current electrodes A-B and potential electrodes M-N was selected after a few in-situ measurements, to obtain a good definition of the apparent resistivity curves. Examples of field measurements are given in Figure 4. The data are plotted using the standard convention for the Schlumberger array, where L = AB/2 and a = MN (distances in meters). These distances between electrode pairs were determined by direct measurement up to 50 m and by topographic survey for larger distances. The uncertainties increased with distance; in general, measurements may be accurate to ± 3.5 %. The uncertainty in the geometric factor K is about 7.9%. Errors due to current and voltage fluctuations, assuming them to be uncorrelated, lead to an apparent resistivity uncertainty of about 8-10% (Bevington, 1969).

The apparent resistivity values were plotted on semilogarithmic paper in the field; this permitted preliminary interpretation and a simple check for possible errors (Del Castillo-García and Urrutia-Fucugauchi, 1975). Qualitative interpretations were based on apparent resistivity (ρa) curve classification and comparison; this may yield resistivity contrasts and depth relationships for some key horizons (Orellana, 1982) All soundings were qualitatively interpreted using a combination of methods including curve matching with catalogues of master curves (Van Dam and Meulenkamp, 1969; Urrutia-Fucugauchi, 1975), auxiliary-point methods (Zhody, 1965; Orellana, 1982) and a computer method based on an iterative algorithm for generating theoretical models (Argelo, 1967; Gosh, 1971; Urrutia-Fucugauchi, 1975). The initial models for interpretation were taken from the preliminary qualitative results. Most of the 300 to 440 m-AB soundings could be approximated by 3 to 4 layer models, but half of the 1000 m-AB soundings suggested more complex structures. Figure 4a illustrates some typical examples of the results and the matching obtained using master curves. This figure also illustrates the overall similarity of resistivity curves along the profile (some 1800 meters in length). Methods of auxilary points were used for interpreting some of the soundings, as well as improving results from the matching procedure (Figure 4b).Finally, the computer program was used for varying the model parameters and exploring alternative models until a close theoretical-to-observed data match was obtained (Figure 4c). Figures 4 to 7 are included to give a feeling for the data and the type of resistivity curves observed, and to illustrate the interpretations.

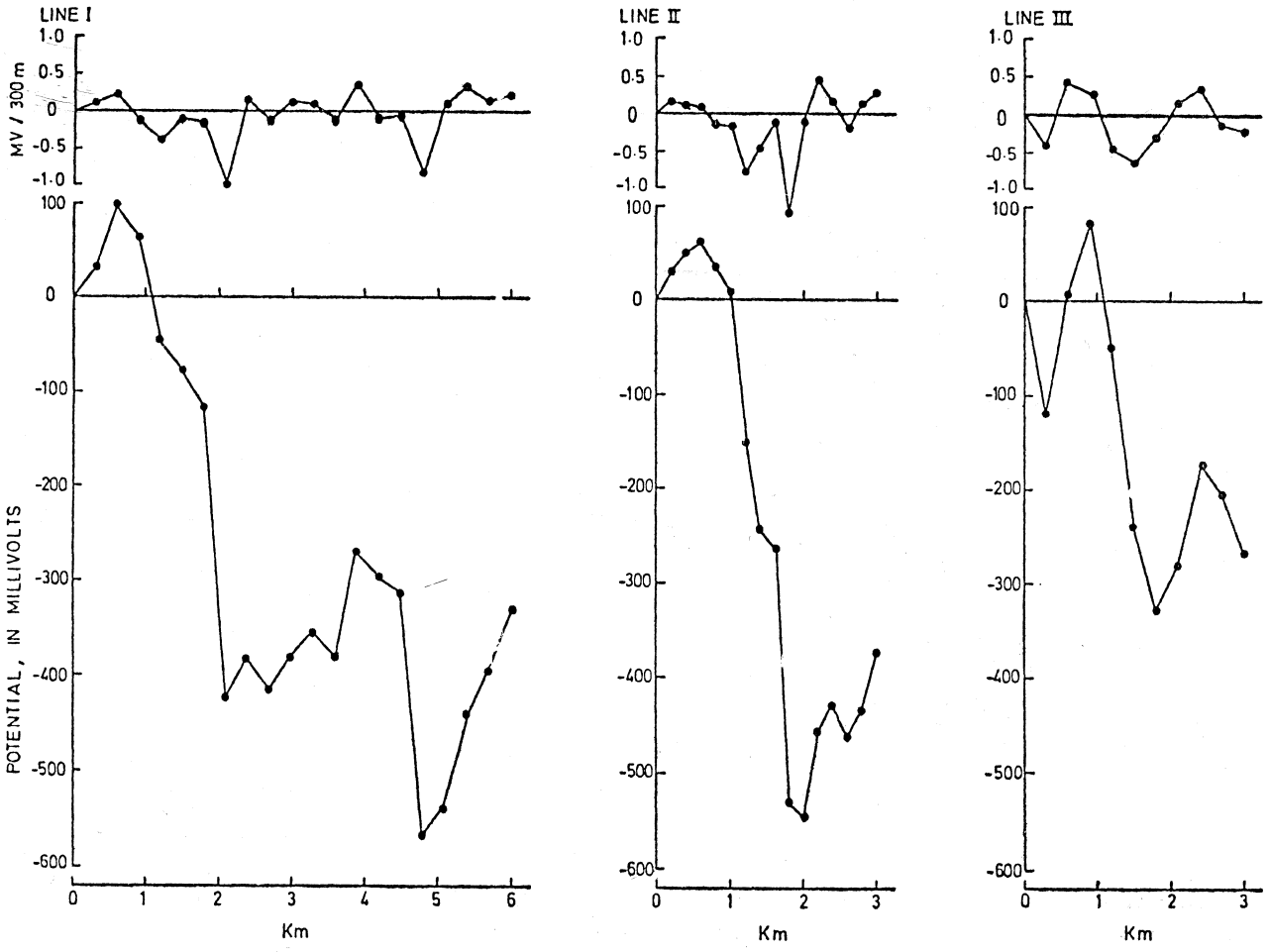

Fig. 3. Summary of self-potential (SP) observations, corresponding to the main profiles: (a) Line I, (b) Line II, diagrams correspond to the horizontal gradient (units in millivolts per 300 meters). Lower diagrams correspond to the average self-potential data (units in millivolts). Note the dipolar-like character of the SP anomalies in all three profiles.

The results were next quantitatively interpreted by inversion using horizontally layered earth models. The theory is given in Lima-Lobato (1979a,b) and Lima-Lobato and Onodera (1980). The methods are based on the application of linear filter theory for fast calculation of apparent resistivity curves. Examples for different types of resistivity field curves are given in Figures 5 to 7.

The results in terms of layer thicknesses and resistivities, i.e. geoelectric sections, are summarized in Figures 8 to 10. These sections are preliminary. In some sections intermediate layers without lateral correlation have been observed. They may represent lateral variations as shown in the geoelectric cross-sections of profile 1-a between soundings 7 and 8 or in profile 2 between soundings 3 and 4 and 5. In the case of profile L-I, the resistivities of layers 4 and 5 are in the range expected for limestones (Parasnis, 1962). They may correlate with the limestone formations (Figure 2). The top layers may correspond to unconsolidated material with varying degree of water saturation; layers 2 and 3 may correspond to the lahar deposits and sediments of the Tlayecac and Cayuca Formations. The anomaly seen near the beginning of L-I seems to correlate well with the trace of the Tlaica anticlinal. It may correspond to fractured limestone with a higher fluid saturation. This may account for the positive self-potential anomaly observed (Figure 3a). Profile L-II shows a surficial layer of alluvium, followed by a layer of clastic material with a high degree of saturation (low resistivities), and the next layers may correspond again to the limestone. In the case of profile L-III, a layer of saturated material and deeper layers of higher resistivity are shown. Notice that the resistivity of granite is usually high, e.g. 5.10^4 Ω-m, which is not reached in this profile, but is observed in L-I and L-II. This may mean that the Jonacatepec granodiorite bodies lie deeper than the depth reached by profile L-III. For profiles L-I and L-II, the high resistivity units are likely to be limestone layers.

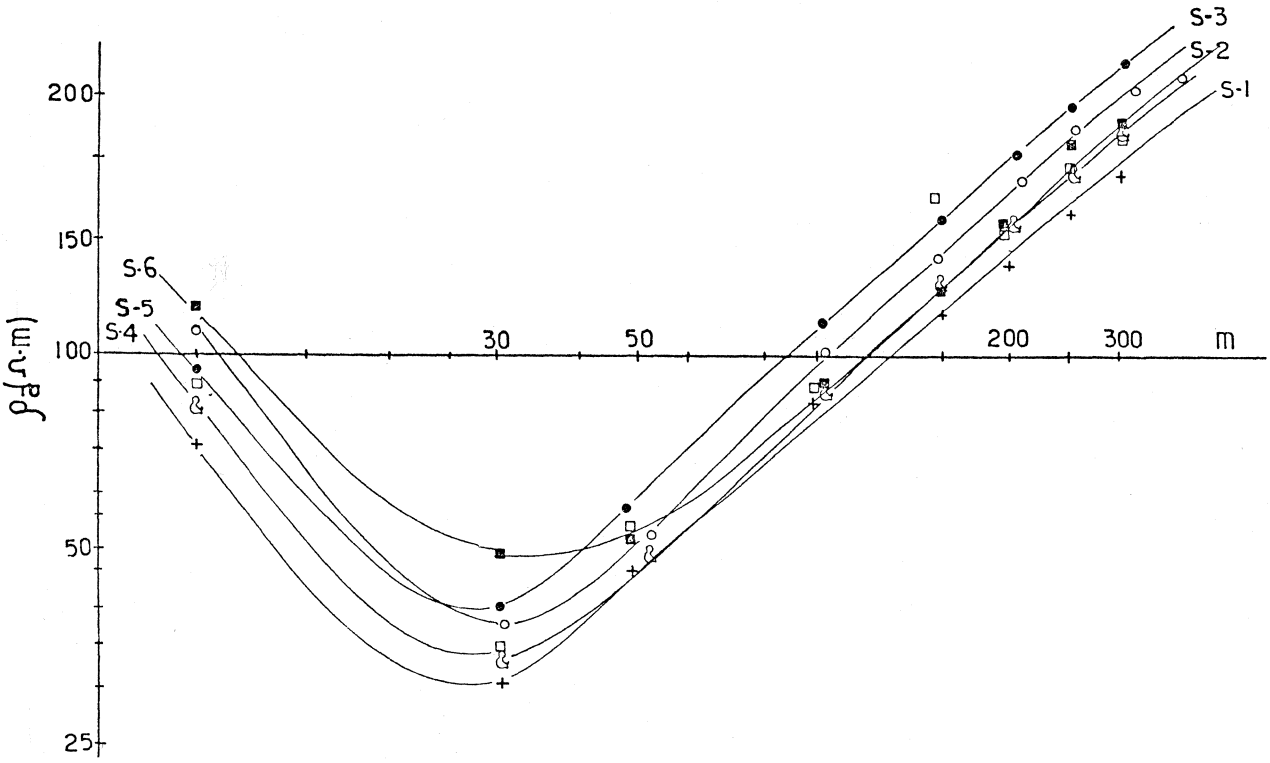

Fig. 4a. Typical examples of curve matching for the interpretation of DC resistivity sounding curves. Electrode configuration is the Schlumberger array. Apparent resistivities (ohm-m) are plotted as a function of half the current electrode distance, AB/2 (meters).

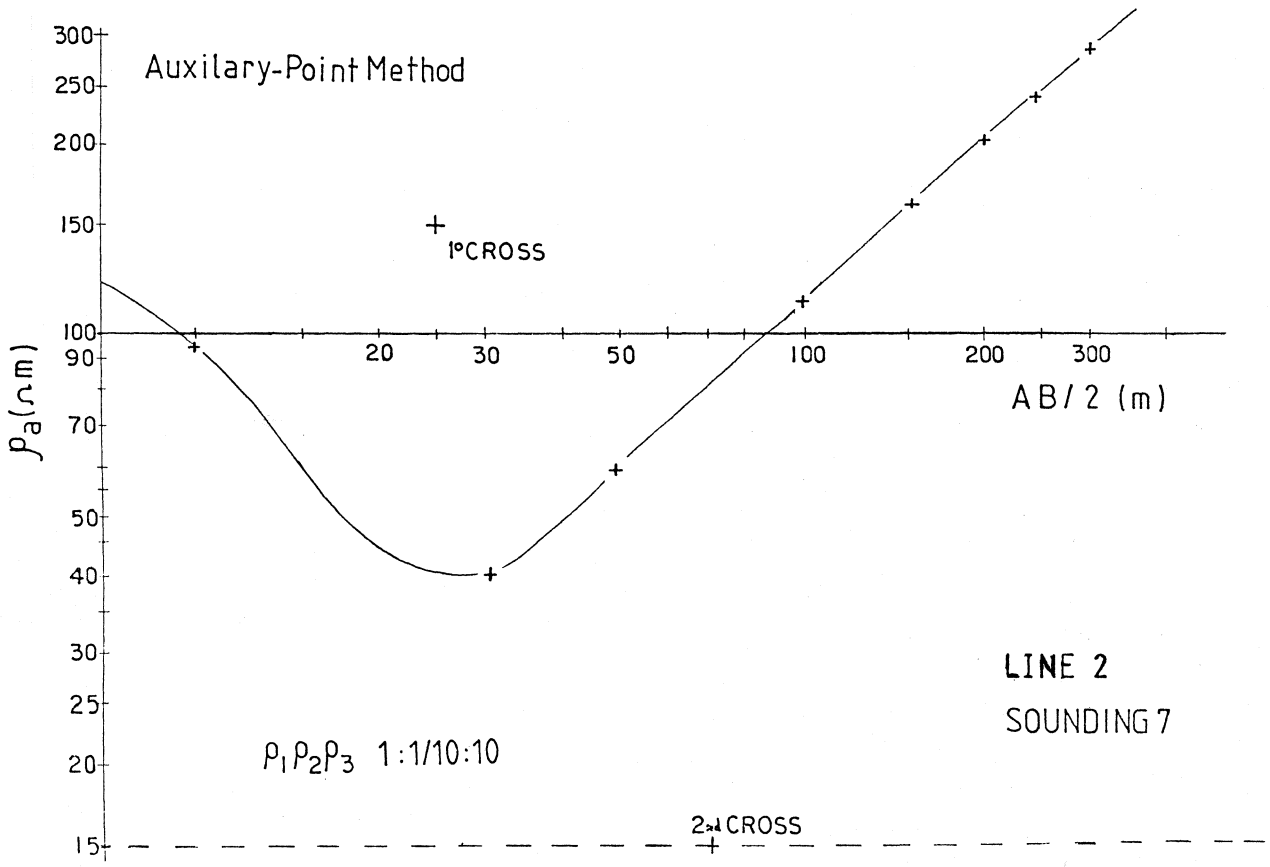

Fig. 4b. Example of modelling using the auxilary-point method.

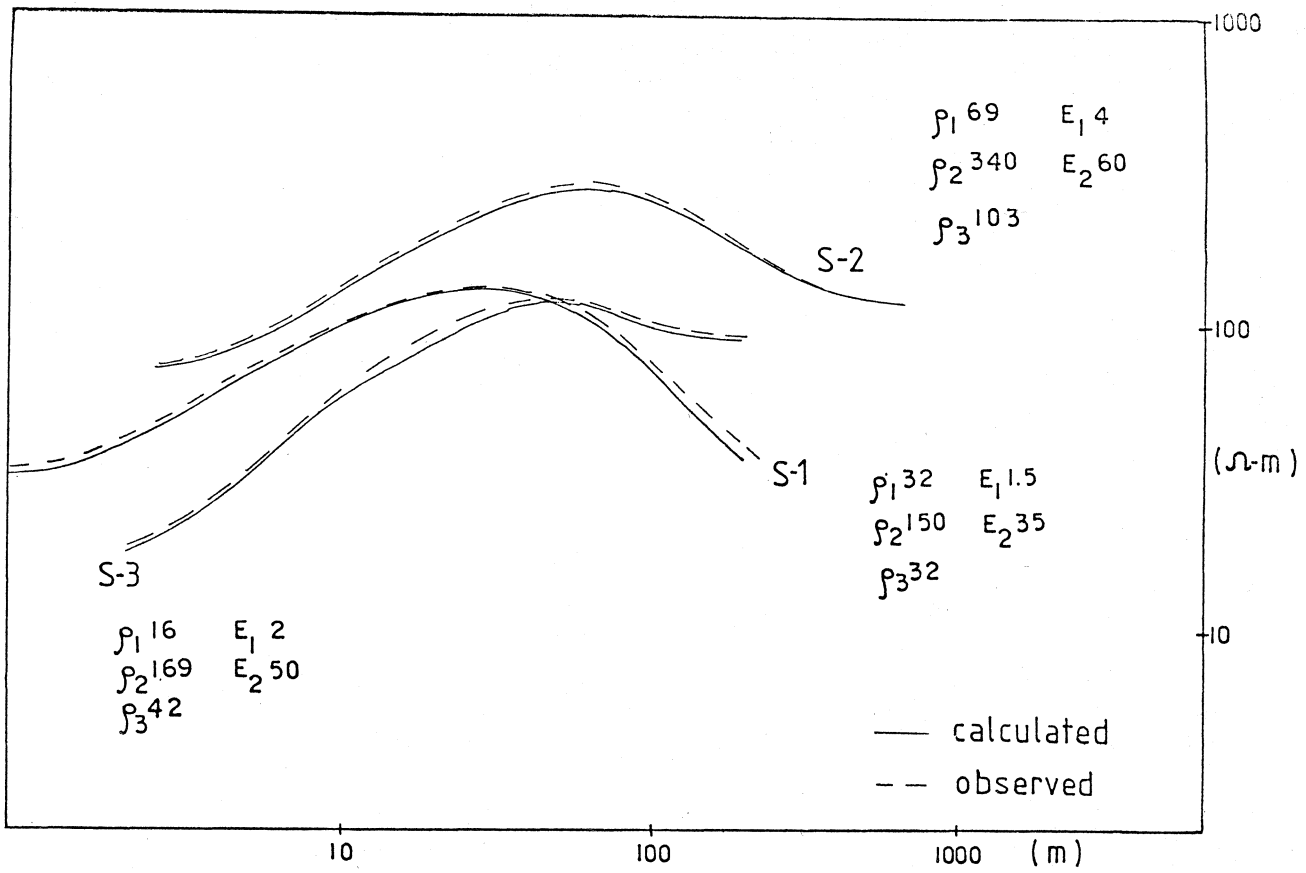

Fig. 4c. Typical examples of interpretation using an iterative algorithm for generating theoretical resistivity curves (dashed curves). Observed data correspond to the continuous curves. Corresponding resistivity and layer thickness values for the synthetic curves are given for the three examples.

DC-SOUNDING OF A LIMESTONE CAVE AND A FAULT ZONE.

A survey over a small shallow limestone cave was conducted as part of the geophysical study in the area, in order to calibrate the electric response of the structure and to investigate the eventual implications, for the interpretation of results. The results show some interesting features which are briefly discussed.

Karstic features of the area include well-developed large caves such as Grutas de Cacahuamilpa and Carlos Pacheco, west of our area. The presence of cavities effectively modifies the conductivity of the limestone units, depending on their size, interconnections, fillings, and fluid content. Caves have however received relatively little attention (e.g. Habberjam, 1969; Del Castillo-García and Urrutia-Fucugauchi, 1975; Militzer *et al.*, 1979). The occurrence of fracturing may result in secondary porosity and permeability of the limestone units. A number of factors controls the response for geoelectrical resistivity, e.g. geometry, alterations and infillings, saturation degree, and salinity (Orellana, 1982). Thus in order to complete the geoelectrical resistivity survey, we also conducted a survey over a limestone cave and in a fault zone, using the Schlumberger electrode configuration in horizontal operational mode.

The area lies to the east of Cocoyoc (Figure 11). The cave was explored before the geoelectrical sounding. It was selected for its relatively small size compared with the maximum electrode arrays allowed by the topography. The maximum AB distance was 200 meters. The measuring electrodes with MN equal to 10 m were horizontally displaced within the middle third of the AB distance. The section of the cave lies within this interval. An example of the results is shown in Figure 12. The high apparent resistivities observed near the central part are attributed to the cavity, which works as a perfect insulator. The top of the cave lies a few meters beneath this area of high resistivity (4 meters). Attempts to detect a possible deeper continuation of the cavity (not accesible from the surface) proved unsuccessful as very low apparent resistivities were measured (less than 10 ohms-m). The cavity lies approximately between points 15 and 30 in the apparent resistivity graph (Figure 12).

A vertical Schlumberger sounding was next conducted over an area of Cañón de Lobos near Olintepec. This narrow pass corresponds to a major fault which trends NW-SE, almost normal to the inferred lateral fault of

CAPA	RES.	ESP.
1	47.020	2.550
2	172.000	16.000
3	66.000	43.000
4	35.000	

AB/2	RES. AP. CAMPO	TEORICA
2	47.500	49.819
3	56.400	54.589
4	62.750	61.181
5	76.930	66.359
6	73.450	75.381
8	84.400	87.846
10	94.200	97.934
13	106.120	109.214
16	125.130	120.370
25	127.560	125.366
30	115.900	124.274
35	119.300	120.979
40	123.150	116.470
50	117.800	106.170
65	99.550	91.519
80	76.400	79.666
100	67.540	67.976
125	56.450	56.111

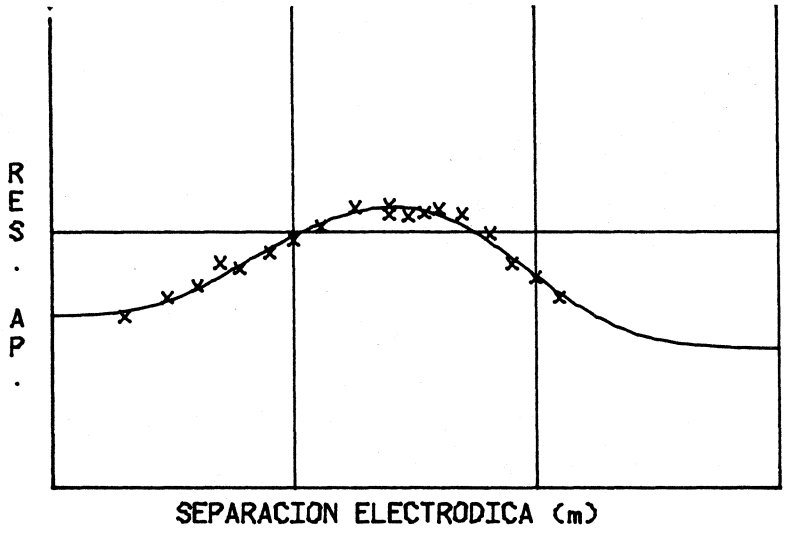

PROYECTO : JONACATEPEC
LINEA : 1
ESTACION : 1

CAPA	MODELO RES.	ESP.
1	20.120	3.060
2	174.690	29.690
3	69.740	76.010
4	79.910	

AB/2	RES. AP. CAMPO	TEORICA
2	19.620	21.466
4	29.100	26.447
6	40.700	34.100
10	62.600	49.916
16	58.000	74.427
25	76.540	89.292
35	101.970	103.271
50	126.400	113.362
80	120.130	113.315
100	112.310	107.698
125	95.720	100.566
150	95.720	94.436

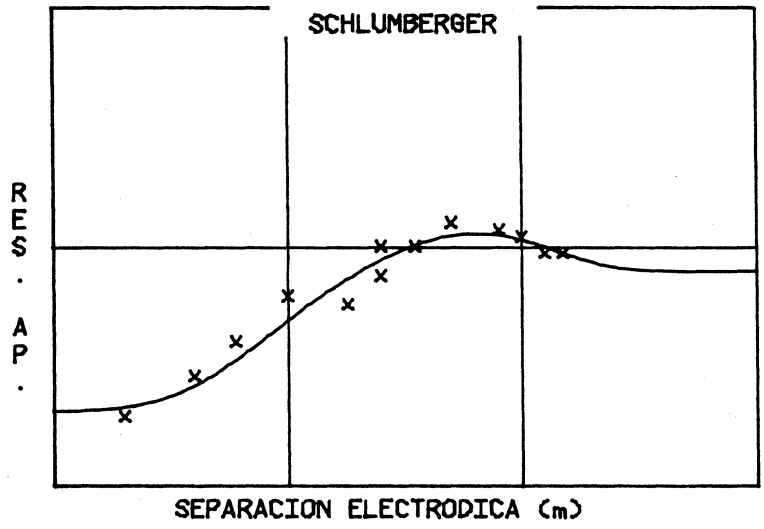

PROYECTO : JONACATEPEC
LINEA : 1
ESTACION : 3

Fig. 5. Typical examples of interpretation for first part ot Line I, using the inversion technique. Observed data points are indicated by the crosses and best-fitting theoretical model is the continuous curve. The two tables on the left-hand side of each diagram give the numerical data. First the details of the best-fitting geoelectric model with the number of layers, the apparent resistivities and the layer thichness. Second, comparison of the observed data (campo) with the calculated data (teorica)tabulated as a function of half the electrode separation (AB/2). See Fig. 10 a for the interpreted geoelectrical cross section and text for discussion.

CAPA	MODELO RES.	ESP.
1	12.020	1.610
2	137.110	30.690
3	126.830	78.020
4	92.710	

AB/2	RES. AP. CAMPO	TEORICA
2	14.370	14.979
4	25.100	23.337
6	33.900	32.107
10	47.100	48.988
18	64.100	68.474
25	80.500	81.502
30	85.500	88.618
35	91.400	94.362
50	111.900	108.154
80	120.600	118.653
100	125.700	119.200
125	135.000	120.083
150	108.030	119.511

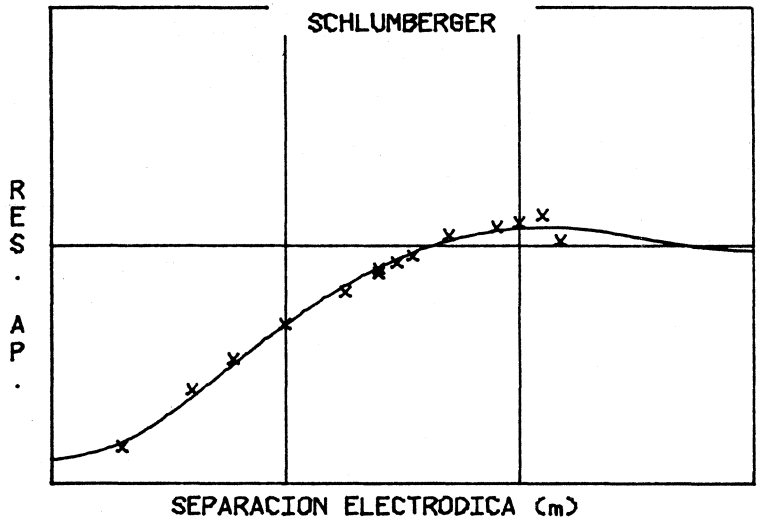

PROYECTO : JONACATEPEC
LINEA : 1
ESTACION : 5

CAPA	MODELO RES.	ESP.
1	24.000	3.000
2	112.000	90.000
3	87.000	

AB/2	RES. AP. CAMPO	TEORICA
2	27.500	25.879
4	28.100	30.901
6	45.200	38.184
10	53.400	51.911
18	70.700	70.600
25	80.400	80.736
30	79.900	85.888
35	82.700	89.871
50	141.400	97.480
80	105.500	103.596
100	108.400	104.806
125	98.200	104.858
150	95.400	104.862

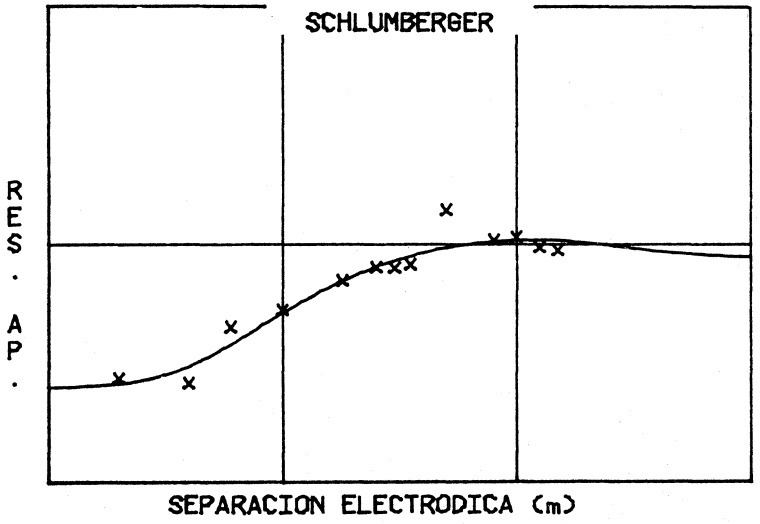

PROYECTO : JONACATEPEC
LINEA : 1
ESTACION : 8

Fig. 5. (Cont.)

CAPA	MODELO RES.	ESP.
1	40.670	2.030
2	132.990	9.000
3	146.630	72.660
4	53.560	

AB/2	PES. AP. CAMPO	TEORICA
2	43.750	44.924
3	50.900	51.058
4	55.300	56.199
6	69.500	71.499
10	86.350	90.501
16	118.500	111.866
25	123.600	120.646
30	118.800	125.085
40	133.200	130.541
50	137.400	133.249
60	140.700	132.693
100	117.600	128.529
125	126.000	120.745
150	157.300	112.818
200	79.800	90.157

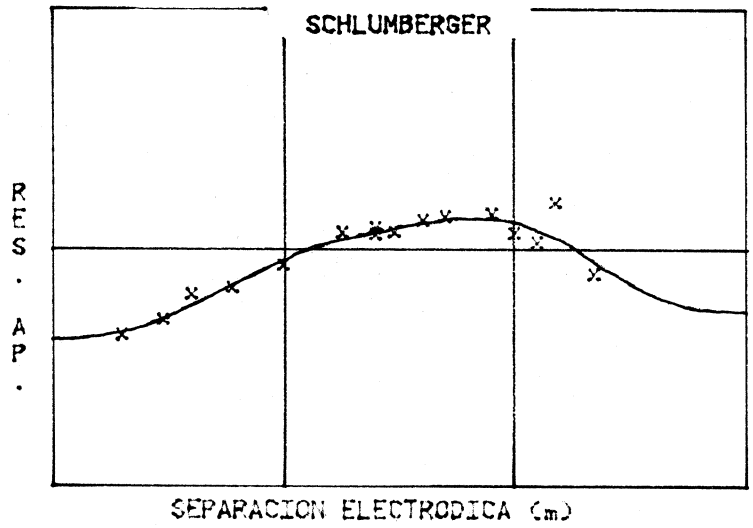

PROYECTO : JONACATEPEC
LINEA : I
ESTACION : 14

CAPA	MODELO RES.	ESP.
1	14.220	1.940
2	106.920	16.160
3	126.940	37.980
4	115.950	

AB/2	RES. AP. CAMPO	TEORICA
2	17.500	16.647
3	19.000	20.463
4	25.100	24.743
6	33.900	33.094
10	47.100	46.776
16	67.100	65.251
25	73.000	75.943
30	80.600	81.764
40	89.200	93.551
50	96.200	96.840
60	125.600	107.650
100	127.200	111.261
125	109.200	113.606
150	109.600	115.158

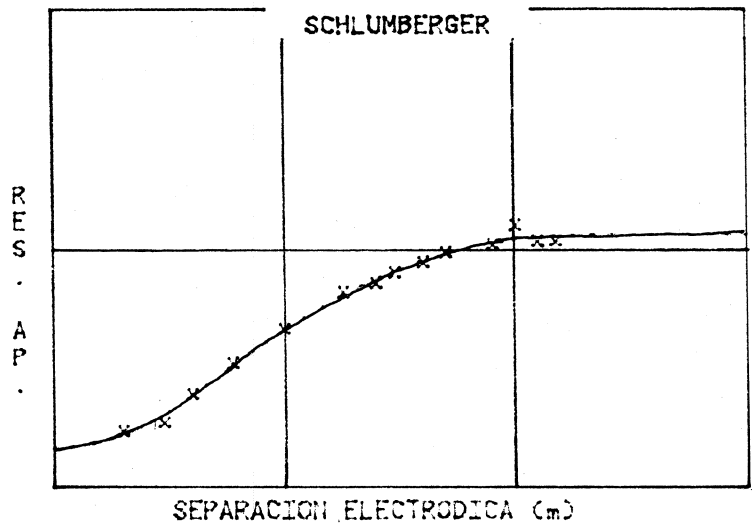

PROYECTO : JONACATEPEC
LINEA : I
ESTACION : 15

Fig. 6. Typical examples of interpretation for the second part of Line II, using the inversion technique for three and four multilayer earth models. See caption of Fig. 7 for explanation. Interpreted geoelectric cross section is given in Fig. 10b.

MODELO

CAPA	RES.	ESP.
1	212.730	2.130
2	595.170	7.410
3	144.350	10.140
4	97.130	40.940
5	617.560	

AB/2	RES. AP. CAMPO	TEORICA
2	212.500	227.966
3	263.000	253.472
4	271.000	282.791
6	339.000	334.102
10	439.600	387.176
16	395.000	366.153
25	274.750	325.151
30	304.010	264.859
40	263.670	284.221
50	149.230	171.545
60	140.740	157.294
100	157.060	173.569
125	171.610	200.360
150	266.610	226.117
200	374.590	279.662

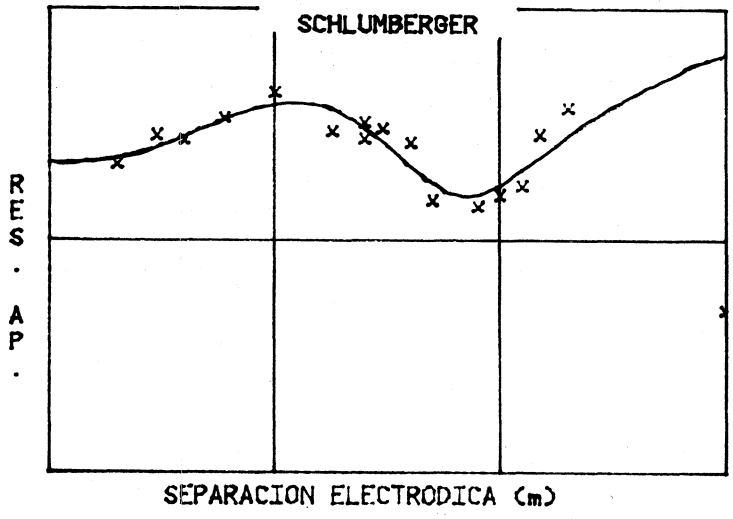

PROYECTO : JONACATEPEC
LINEA : 2
ESTACION : 1

MODELO

CAPA	RES.	ESP.
1	358.860	1.420
2	748.730	4.760
3	88.960	36.040
4	676.600	

AB/2	RES. AP. CAMPO	TEORICA
2	356.250	407.446
3	466.950	456.000
4	602.400	493.607
6	546.250	526.729
10	455.300	422.871
16	226.900	277.271
25	196.250	179.665
30	176.100	146.196
40	113.850	123.218
50	111.610	126.136
60	155.660	161.983
100	172.760	169.381
125	333.760	238.381
150	280.140	302.215

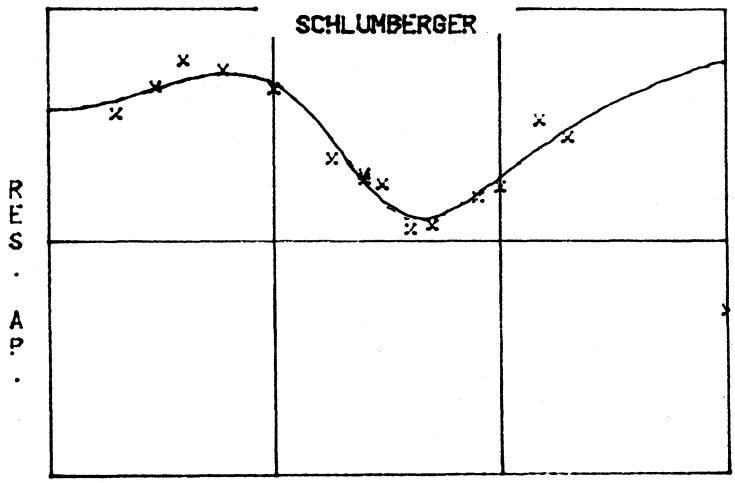

PROYECTO : JONACATEPEC
LINEA : 2
ESTACION : 3-N

Fig. 7. Typical examples of interpretation for Line II, using the inversion technique for three and four multilayer earth models. See Fig. 7 for explanation. Interpreted geoelectric cross section is given in Fig. 11. See text for discussion.

MODELO CAPA	RES.	ESP.
1	464.320	6.400
2	66.760	34.560
3	622.590	

AB/2	RES. AP. CAMPO	TEORICA
2	365.250	462.766
3	466.950	460.666
4	602.400	476.213
6	548.250	461.226
10	455.300	404.773
16	226.900	263.192
25	196.250	183.503
30	176.750	152.232
40	113.290	127.033
50	117.610	125.976
60	155.600	159.347
100	172.760	165.761
150	333.260	244.753
200	282.740	293.010

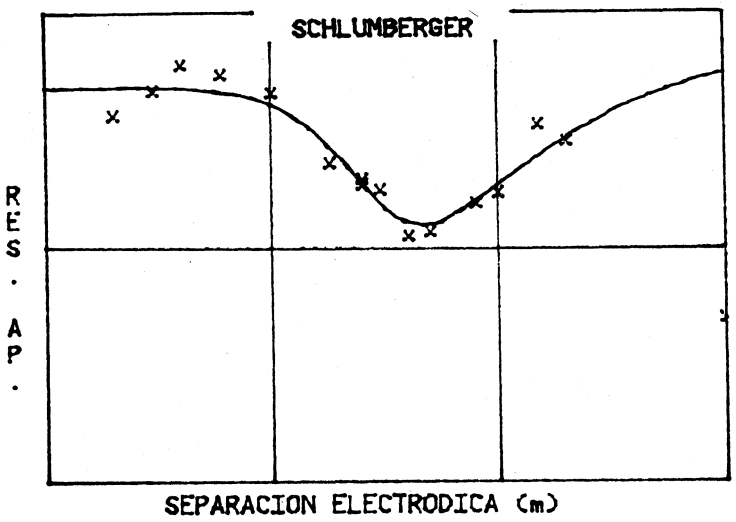

PROYECTO : JONACATPEC
LINEA : 2
ESTACION : 3-M

MODELO CAPA	RES.	ESP.
1	359.150	2.970
2	552.430	10.100
3	129.160	74.560
4	136.670	

AB/2	RES. AP. CAMPO	TEORICA
2	343.750	362.801
3	362.050	372.022
4	356.420	384.592
6	435.050	410.634
10	502.400	441.440
16	366.230	416.229
25	392.500	354.213
30	311.080	309.909
40	251.300	240.366
50	162.970	196.655
60	155.620	147.533
100	172.600	139.673
125	132.700	136.532
150	123.700	135.565
200	138.230	135.102

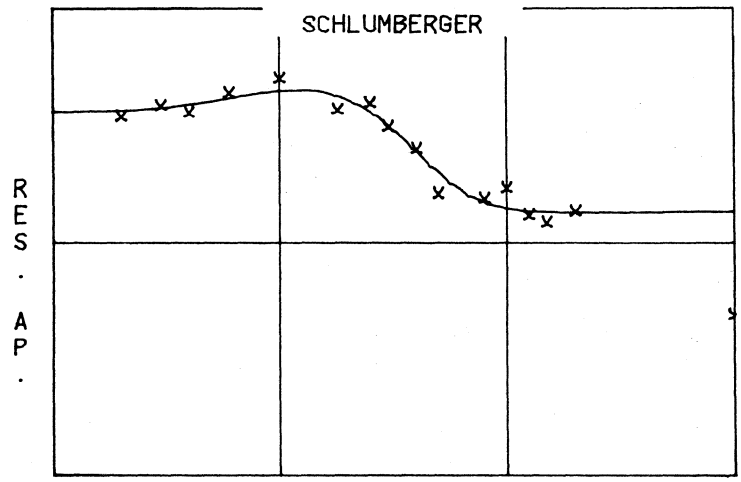

PROYECTO : JONACATEPEC
LINEA : 2
ESTACION : 7

Fig. 7. (Cont.).

Chinameca (Fries, 1965) which crosses the area near the northwest corner (Figure 2). The fault has the same general trend as the folds of the Cretaceous limestones and the continental Lower Tertiary sedimentary deposits. The sounding was conducted over alluvium in a flat-lying plain. It is at right angles to the inferred trace of the fault. The DC sounding yields low apparent resistivity values, in the order of 10 ohms-meter and a flat curve. The low values and no-contrast curve are interpreted as due to enhanced conductivity close to the fault. Uncertainties in the location and extent of the fractured region and subsurface structure do not allow a quantitative interpretation or inferences concerning the electrical resistivity features.

DISCUSSION

The preliminary results successfully outline the shallow structure of the volcanoclastic, alluvial and lahar units and provide constraints on the intrusive bodies. Most Schlumberger DC soundings can be modelled by 3 to 4 layer sections. Apparent resistivities of the layers vary among profiles, but there is an overall continuity among profiles. The surficial layer corresponds to unconsolidated material with varying degrees of water saturation. Intermediate layers 2 and 3 may correspond to lahar deposits and sediments of the Tlayecac and Cayuca formations. Deeper layers 4 and 5 may correspond to the limestone units. The subsurface continuation of the Jantetelco intrusive bodies lies deeper than about 150 meters.

As to the geothermal potential of the area, the results (though inconclusive) suggest dipolar self-potential anomalies in certain areas which may be associated with geothermal sources. More studies are required using self-potential and resistivity methods in order to understand the shallow underground structure and the origin and nature of the SP anomalies.

The uncertainties involved in the present interpretation are high, especially because of the non-uniqueness of the resistivity models.

The nature and origin of self-potential anomalies over geothermal areas are not fully understood at present. Surveys have reported different types of anomalies of varying amplitude; for instance, negative anomalies have been found in the Dunes thermal area, California (Combs and Wilt, 1976) in the Leach Hot Spring area, in Grass Valley, Nevada, in the Cerro Prieto geothermal area, Mexico (Corwin and Hoover, 1979; Fitterman and Corwin, 1982), and in the Otake geothermal field, Kyushu, Japan (Onodera, 1974). Positive anomalies have been found in Parbati Valley, India (Jangi *et al.*, 1976), on Kilauea volcano, Hawaii (Zablocki, 1976) and in the Mud Volcano area, Yellow-stone Park (Zohdy *et al.*, 1973). Dipolar anomalies have been found in Long Valley, California (Anderson and Johnson, 1976), Raft Rifer Valley, Idaho (Mabey *et al.*, 1978) and Mono Lake, California (Corwin and Hoover, 1979). Aubert and Lima-Lobato (1986) report large positive SP anomalies for the northern slope of the Volcán de Fuego, Colima, associated with hydrothermal activity in a highly fractured zone.

Results from a simultaneous rock-magnetic and palaeomagnetic study (Urrutia-Fucugauchi, 1981) provide some constraints on the nature and features of the intrusive bodies. Some of those results are summarized here. Location of sampling sites is shown in Figure 2a. The polarity of the geomagnetic field at the time of the remanence acquisition of the lavas (Tepexco Volcanic Group) was reversed. The intrusive granodiorites are piercing through the lavas, so presumably the geomagnetic field at the time of remanence acquisition was like that after the emplacement of the lavas. Samples from one of the sites (JG6) seem to record a polarity transition (marked by two characteristic remanence components). The remaining four sites show a field of normal polarity; these correspond to the largest body. Rock magnetic data show no major differences between the results from the several bodies; this is in agreement with field and petrographic observations.

Everything suggests that the bodies belong to a single major intrusive. The differences in remanence directions may be due to geomagnetic field variations with time, related to the cooling process of the intrusive body. The sites JG5-7 may be located closer to the edges of the body than sites JG1-4, which are near the center of the intrusive.

A more detailed study may disclose the thermal conditions prevailing within the body today. For instance, the cooling of one of the specimens (2.5 cm diameter, 2.3 cm height) from site JG6 (about 580°C to about 200-300°C) spanned one reversal of the Earth's magnetic field. Assuming an average duration for polarity chrons during the Tertiary (e.g. Cox, 1982) we obtain a cooling rate of about 5.6° to 7.6°C/Ma. These rates are compatible with a large intrusive body as suggested in this paper. Thus the Jantetelco bodies would represent the surface expressions of a deeper and larger igneous body.

ACKNOWLEDGMENTS

Useful comments and assistance with modelling of DC vertical soundings and SP data by Enrique Lima Lobato are gratefully acknowledged. Part of the data processing and modelling of the vertical resistivity soundings was provided by Martin Bremer Bremer. Most of the field survey was completed as part of course in "Electrical Prospecting" for the Earth Sciences Division, Faculty of Engineering, UNAM. The assistance of the students, and of Carlos Flores L. and Octavio Orozco F., in the field work and the preliminary data processing is gratefully acknowledged. The friendly cooperation of local authorities and residents, and in particular from Jonacatepec Village, proved invaluable for development of the project.

Assistence with the preparation of the manuscript by Lucía Castrejón is gratefully acknowledged. Useful discus-

sions with J. F. W. Negendank, Harald Böhnel, Dante J. Morán, Oscar Campos and Julio César García on the geology and paleomagnetic data were helpful in developing this work. A useful review of the manuscript was provided by Oscar Campos Enríquez. Comments by two journal reviewers are also acknowledged.

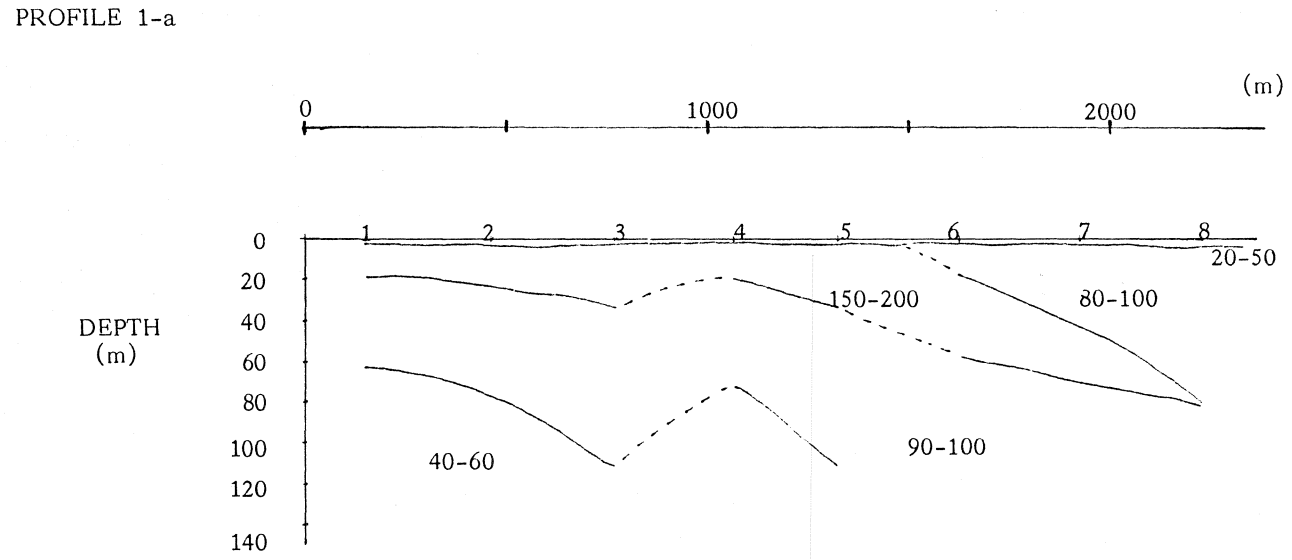

Fig. 8 (a). Interpreted geoelectric cross section for Line I. (a) first part of profile.

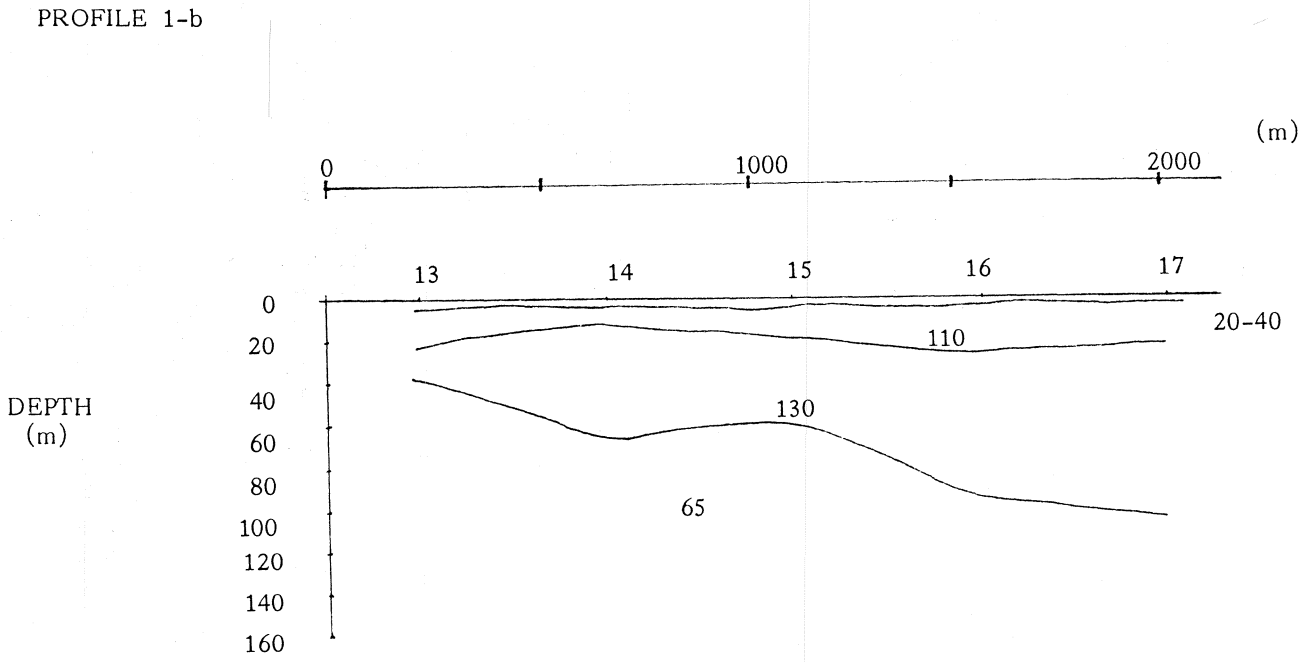

Fig. 8 (b). Second part of profile. Horizontal distance and depth in meters. Apparent resistivity values for modelled layers in ohm-m. Numbers along the line (1 to 8) correspond to sounding identification.

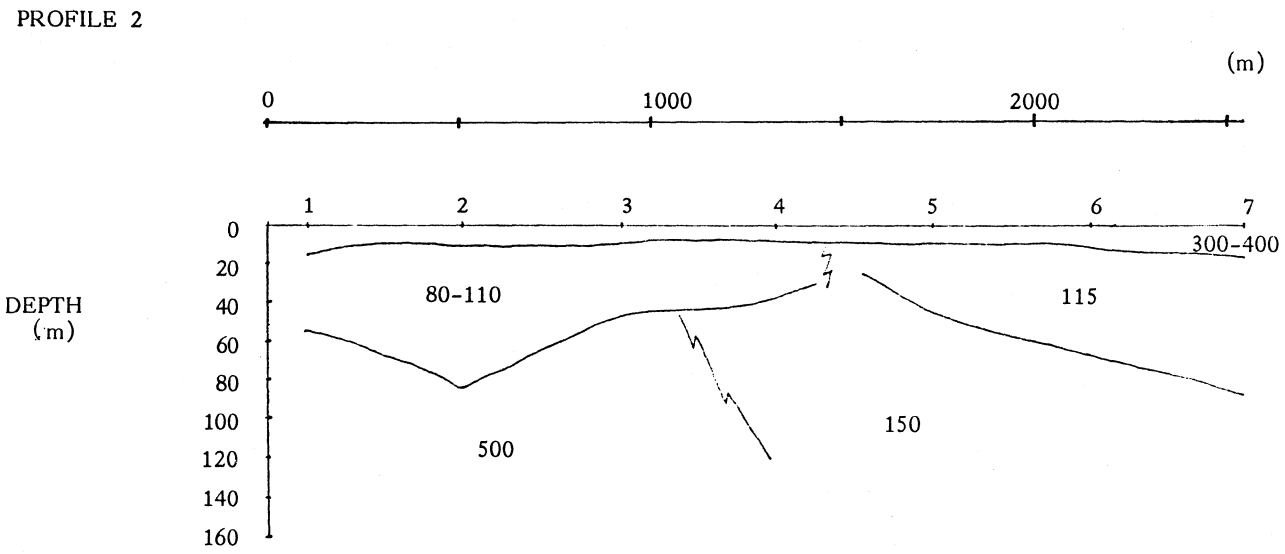

Fig. 9. Interpreted geoelectric cross section for Line II. See caption of Fig. 10 for explanation.

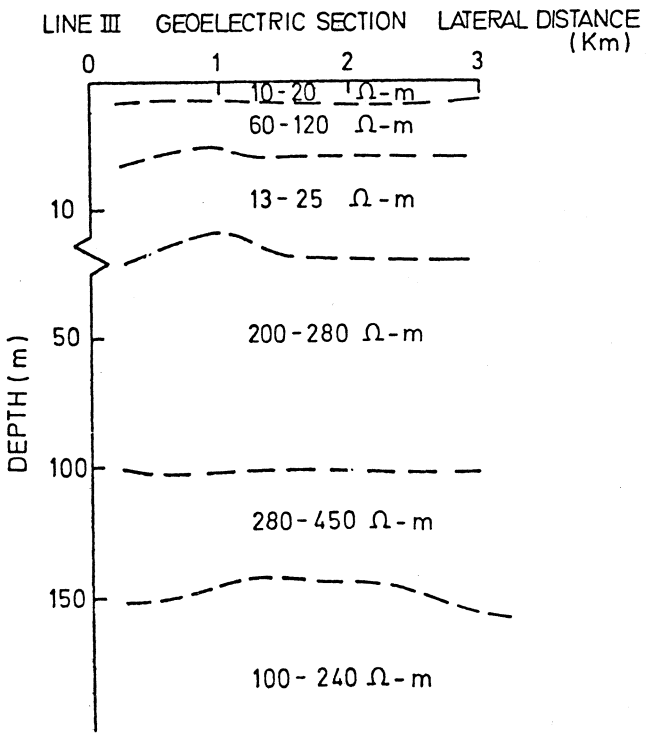

Fig. 10. Interpreted geoelectric cross section for Line III. Horizontal distance in kilometers and depths in meters. Note the break in scale for the depths which is only for clear graph ical display of the shallow layers along the section.

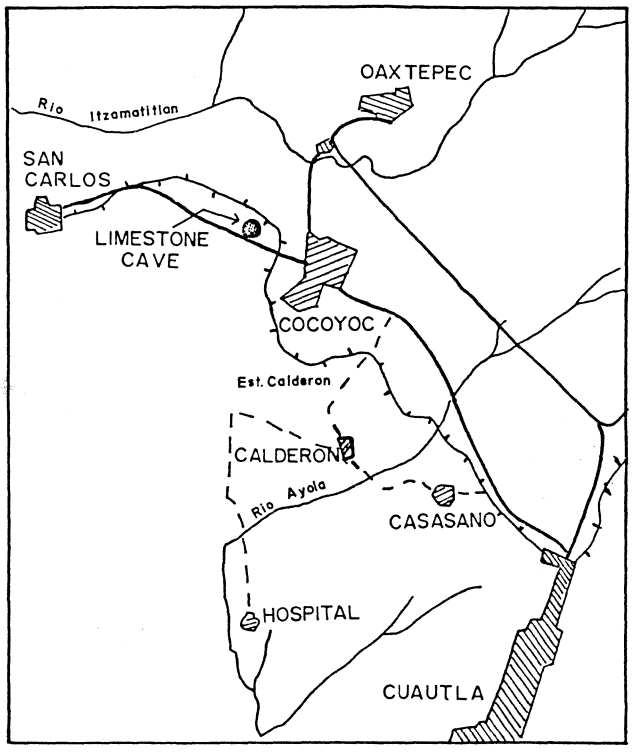

Fig. 11. Schematic map showing location of the Cocoyoc limestone cave sounding. Area lies to the west of the main study area of Atotonilco-Jonacatepec. See text.

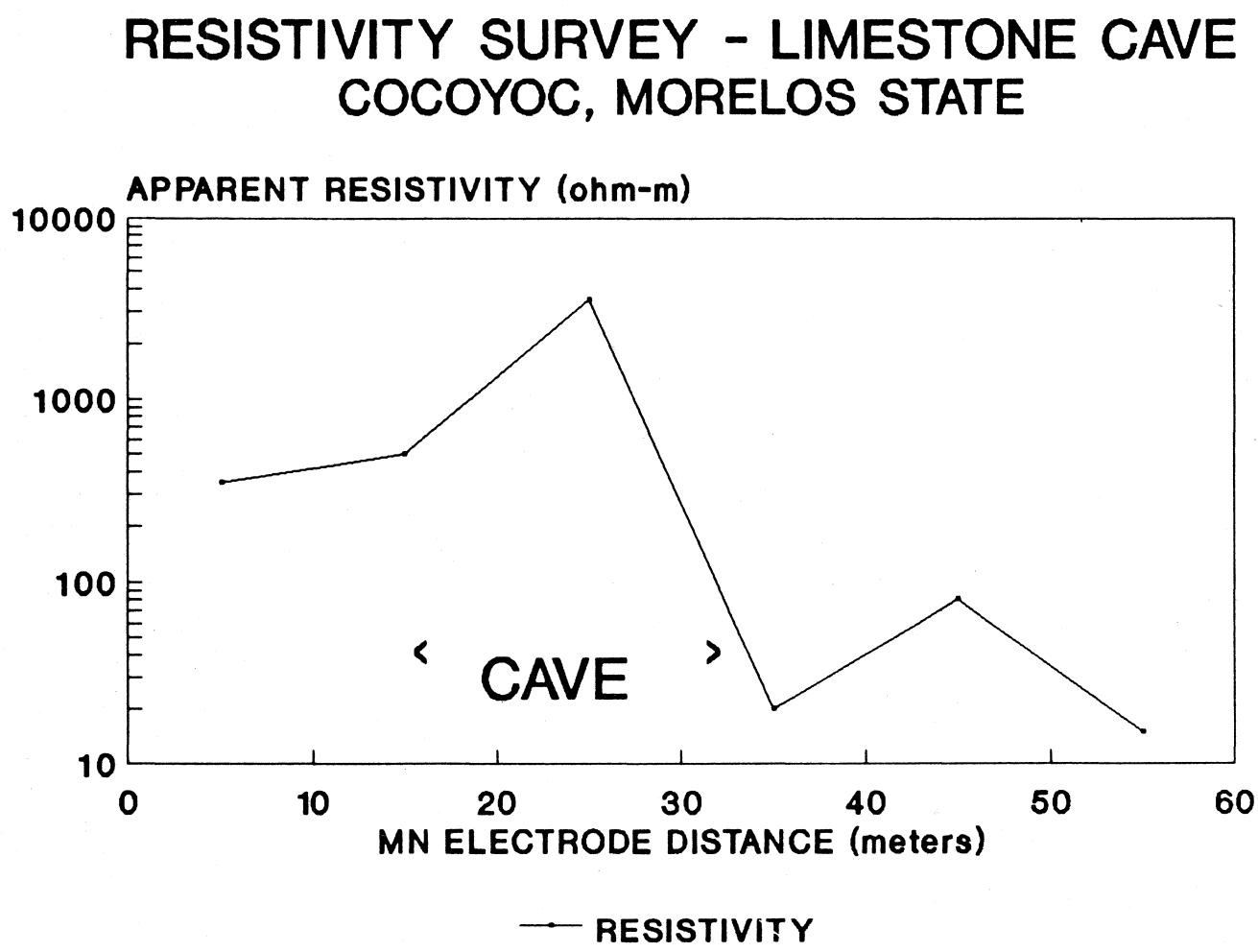

Fig. 12. DC horizontal resistivity curve observed across the limestone cave. Electrode configuration used for the horizontal sounding is the Schlumberger. See text for discussion.

BIBLIOGRAPHY

ANDERSON, L. A. and G. R. JOHNSON, 1976. Application of the self-potential method to geothermal exploration in Long Valley, California. *J. Geophys. Res., 81* (8), 1527-1532.

ARGELO, 1967. Two computer programs for the calculation of standard graphs for resistivity prospecting. *Geophys. Prosp., 15*, 71-91.

AUBERT, M. and E. LIMA-LOBATO, 1986. Hydrothermal activity detected by self-potential measurements at the N-S volcanic axis between the volcanoes "Nevado de Colima" and "Volcán de Fuego de Colima" (Mexico). *Geof. Intern., 25*, 575-586.

BEVINGTON, P. R., 1969. Data reduction and error analysis for the physical sciences. McGraw-Hill Book Co., N. Y.

COMBS, J. and M. WILT, 1976. Telluric mapping, telluric profilling, and self-potential surveys of the Dunes geothermal anomaly, Imperial Valley, California. *In:* Proc. 2nd U. N. Symp. Development and Use of Geothermal resources, San Fco. California, 2, 917-928.

CORWIN, R. F. and D. B. HOOVER, 1979. The self-potential method in geothermal exploration. *Geophys., 44*, 226-245.

COX, A., 1982. Magnetostratigraphy. *In:* Geological Time Scale, Cambridge University Press, Cambridge, UK

DE CSERNA, Z., 1965. Reconocimiento geológico en la Sierra Madre del Sur de México, entre Chilpancingo y Acapulco, Estado de Guerrero. Bol. Inst. Geol., UNAM, 62, 76 pp.

DEL CASTILLO-GARCIA, L. y J. URRUTIA-FUCUGAUCHI, 1975. Sondeos eléctricos practicados en el Fraccionamiento Bosques de Reforma, México, D. F. Technical Report SOLUM, S. A., México, D. F. 21 pp + Appendix.

FITTERMAN, D. V. and R. F. CORWIN, 1982. Inversion of self-potential data from the Cerro Prieto geothermal field, Mexico. *Geophys., 47,* 938-945.

FRIES, C., 1960. Geología del Estado de Morelos y de partes adyacentes de México y Guerrero, región central meridional de México. Bol. Inst. Geol., UNAM, 60, 236.

FRIES, C., 1965. Geología de la Hoja Cuernavaca, Estados de Morelos, México, Guerrero y Puebla. Inst. Geol., UNAM, Geol. Map and Text, 14 Q-h (18), Scale 1:100 000, México.

GOSH, D. P., 1971. Inverse filter coefficients for the computation of apparent resistivity standard curves for horizontally stratified earth. *Geophys. Prosp., 19,* 769-775.

HABBERJAM, G. M., 1969. The location of spherical cavities using a tripotential resistivity technique. *Geophys. 34,* 780-785.

JAFFE, H. W., D. GOTTFRIED, C. L. WARING and H. W. WORTHING, 1959. Lead-alpha age determinations of accessory minerals of igneous rocks (1953-1957) US Geol. Surv. Bull., 1097-B, 65-148.

JANGI, B. L., G. PRAKASH, K. J. S. DUA, J. L. THUSSU, D. B. DIMRI and C. S. PATHAK, 1976. Geothermal exploration of the Parabati Valley geothermal field Kulu District, Himachal Pradesh, India. *In:* Proc. 2nd U. N. Symp. Development and Use of Geothermal Resources, San Fco. California, 2, 1085-1094.

KELLER, G. V. and F. C. FRISCHKNECHT, 1966. Electrical methods in geophysical prospecting. Pergamon Press, Oxford, UK, 519.

KUNETZ, G., 1966. Principles of direct current resistivity prospecting. Gebrüder Borntraeger, Berlin-Nikolassee, 103.

LIMA-LOBATO, E., 1979a. A new method for the calculation of apparent resistivity curves of horizontally multilayered models. Mem. Fac. Engineering, Kyushu Univ., Japan, 39, 115-128.

LIMA-LOBATO, E., 1979b. Deriving recurrence formulas for the eigenfunctions for each layer of horizontally multi-layered earth models. Mem. Fac. Engineering, Kyushu Univ., Japan, 39, 183-192.

LIMA-LOBATO, E. and S. ONODERA, 1980. Matching Kernel function curves in order to interpret field resistivity data. Mem. Fac. Engineering, Kyushu Univ., Japan, 40, 133-148.

LINARES, E. and J. URRUTIA-FUCUGAUCHI, 1981. On the age of the Riolita Tilzapotla volcanic activity and its stratigraphic implications. Isochron West, 32, 5-6.

MABEY, D. R., D. B. HOOVER, J. E. O'DONNELL and C. W. WILSON, 1978. Reconnaissance geophysical studies of the geothermal system in the southern Raft Valley, Idaho. *Geophys., 43,* 1470-1484.

MILITZER, H., R. ROSLER and W. LOSCH, 1979. Theoretical and experimental investigations for cavity research with geoelectrical resistivity methods. *Geophys. Prosp., 27,* 640-652.

ONODERA, S., 1974. Geoelectric indications at the Otake geothermal field in the western part of the Kujyu Volcano group, Kyushu, Japan. *In:* The utilization of Volcano Energy, Sandia Lab., Albuquerque, New Mexico, USA, 80-106.

ORELLANA, E., 1982. Prospección Geoeléctrica en corriente contínua. 2nd Ed., Ed. Paraninfo, Madrid, España, 578 pp.

STANLEY, W. D., D. B. JACKSON, and A. A. R. ZOHDY, 1976. Deep electrical investigations in the Long Valley geothermal area, California. *J. Geophys. Res., 81,* 810-820.

TRIPP, A. C., S. H. WARD, W. R. SILL, C M. SWIFT and W. R. PETRICK, 1978. Electromagnetic and Schlumberger resistivity sounding in the Roosevelt Hot Spring KGRA. *Geophys., 43,* 1450-1469.

URRUTIA-FUCUGAUCHI, J., 1975. Prospección Geoeléctrica. Notas Curso de Prospección Eléctrica, Fac. Ing., UNAM, México.

URRUTIA-FUCUGAUCHI, J., 1981. Palaeomagnetism of the Miocene Jantetelco Granodiorites and Tepexco Volcanic Group and inferences for crustal block rotations in Central Mexico. *Tectonophys., 76,* 149-168.

URRUTIA-FUCUGAUCHI, J., 1983. Preliminary palaeomagnetic study of lower Tertiary volcanic rocks from Morelos and Guerrero States. *Geof. Intern., 22,* 87-110.

VAN DAM, J. C. and J. J. MEULENKAMP, 1969. Standard graphs for resistivity prospecting. European Assoc. Expl. Geophys., The Netherlands.

ZABLOCKI, C. J., 1976. Mapping thermal anomalies on an active volcano by the self-potential method, Kilauea, Hawaii. *In:* Proc. U. N. Symp.Development and Use of Geothermal Resources, San Fco. California, 2, 1299-1309.

ZOHDY, A. A. R., 1965. The auxiliary point method of electrical sounding interpretation and its relationship to the Dar Zarrouk parameters. *Geophys., 30,* 644-660.

ZHODY, A., A. R., L. A. ANDERSON and L. J. P. MUFFLER, 1973. Resistivity, self-potential and in duced-polarization surveys of a vapor dominated geothermal system, *Geophys., 38,* 1130-1144.

J. Urrutia-Fucugauchi
Instituto de Geofísica, UNAM
Cd. Universitaria
04510 México, D.F.